28p

NASA TN D-1643

N63-15347
code-1

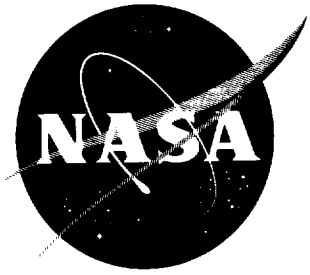

TECHNICAL NOTE

D-1643

CALCULATED RESULTS FOR THE TRANSIENT HEATING AND MELTING PROCESS OF GLASS SHIELDS WITH VARIOUS MATERIAL PROPERTIES AT THE STAGNATION POINT OF A RE-ENTERING ICBM

By John D. Warmbrod

George C. Marshall Space Flight Center
Huntsville, Alabama

NATIONAL AERONAUTICS AND SPACE ADMINISTRATION

WASHINGTON

May 1963

Code-1

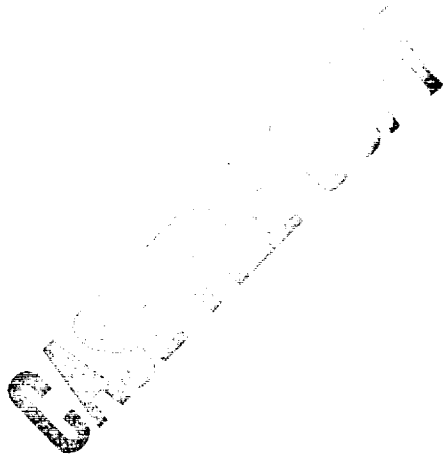

TABLE OF CONTENTS

LIST OF ILLUSTRATIONS

LIST OF TABLES

LIST OF SYMBOLS

Symbol	Unit	Definition
A	-	Level factor in the function for the vapor pressure of the glass
b	mm	Maximum thermal penetration across the shield
c	-	Mass fraction of the injected vapor at the surface
c_p	kcal/kg°K	Specified heat
D	m	Diameter of the spherical body in the vicinity of the stagnation point
h_v	kcal/kg	Heat of Vaporization
h_e	kcal/kg	Enthalpy of air at the outer edge of the boundary layer
h_i	kcal/kg	Enthalpy of air at the interface
H	km	Flight altitude
K_M	-	Dimensionless stagnation point velocity gradient
k	kcal/m°K sec	Thermal conductivity
$k/\gamma c_p$	m^2/sec	Thermal diffusivity
M	-	Molecular weight ratio (air to glass vapor)
Nu	-	Nusselt number
p	kg/m^2	Pressure
Pr	-	Prandtl number
p_v	kg/m^2	Vapor pressure
p_s	kg/m^2	Pressure in the vicinity of the stagnation point
q	$kcal/m^2$sec	Instantaneous heat transfer rate
q_c	$kcal/m^2$	Convected heat flux, i.e., heat carried away by the flow of molten glass given by

$$q_c = - \int_{z=0}^{\infty} \gamma c_p (T - T_0) \frac{\partial v}{\partial Z} \, dz$$

LIST OF SYMBOLS (CONT'D)

Symbol	Unit	Definition
$Q(t)$	$kcal/m^2$	Time integrated heat transfer rate, $Q(t) = \int_0^t q\, dt$
Q_{Bl}	$kcal/m^2$	Total heat blocked per unit area by mass transfer, see equation (14)
R	m	Nose radius of the spherical body in the vicinity of the stagnation point
Re	-	Reynolds number
s	mm	Total ablation, i.e., thickness of glass that ablated away during the re-entry
t	sec	Time scale, t = 0 at H = 150 km
t_f	sec	Impact time
T	°K	Temperature
T_o	°K	Temperature of the glass shield before heating
v_{oo}	mm/sec	Ablation velocity
V_∞	m/sec	Flight speed
z	mm	Axial co-ordinate
α	°	Angle of attack
γ	kg/m^3	Specific weight of the glass
ϵ	-	Emissivity constant of the opaque glass
μ	$kgsec/m^2$	Viscosity
μ^*	-	Level factor in the viscosity function for glass
ρ	$kgsec^2/m^4$	Density
ψ	-	Ratio of aerodynamic heat transfer with and without mass injection

SUBSCRIPTS

i	Pertains to the interface
e	Pertains to the outer edge of the boundary layer
F.S.	Pertains to fused silica (quartz)
P	Pertains to Pyrex glass
∞	Pertains to free stream conditions

NATIONAL AERONAUTICS AND SPACE ADMINISTRATION

TECHNICAL NOTE D-1643

CALCULATED RESULTS FOR THE TRANSIENT HEATING AND MELTING PROCESS OF GLASS SHIELDS WITH VARIOUS MATERIAL PROPERTIES AT THE STAGNATION POINT OF A RE-ENTERING ICBM

By John D. Warmbrod

INTRODUCTION

A ballistic vehicle re-entering the earth's atmosphere at high speeds possesses a large amount of kinetic energy which is converted into aerodynamic heat. The terrific heat which surrounds the missile body requires that the body be coated with some type of material that can withstand this intense heat. Theoretical and experimental investigations have proved that certain type glasses make a very good protective covering for a re-entry vehicle.

For the approximately spherical surface in the vicinity of the forward stagnation point of an ICBM, this report presents calculated results pertaining to the transient heating and ablation processes of 26 homogeneous, opaque, and non-decomposing glass shields, each shield having a unique set of thermal properties. The effect of the thermal properties on the heating and ablation results was investigated by varying each thermal property over a practical range of values. A similar study of the effect of the thermal properties on the heating and ablation results has been made for an IRBM re-entry [1, 4].

The results presented in this report for the ICBM re-entry were obtained by employing the numerical calculation method derived in references 3 or 5 and were evaluated on an IBM 704 computer.

THE TRAJECTORY AND BODY CHARACTERISTICS

The ICBM is assumed to begin its re-entry into the earth's atmosphere at an altitude of 150 km at Mach 15.68 or a flight speed of 7225.9 m/sec. Figure 2 shows the flight altitude and flight speed as a function of time for the ICBM re-entry. The time t = 0 sec corresponds to the altitude of 150 km. The re-entry angle (θ_E) is 114°, measured from the vertical, and the angle of attack (α) that remains constant throughout the re-entry is 0°. The horizontal range of the missile from zero time (H = 150 km) to impact time (H = 0 km) is 330.3 km. The ballistic factor (c_B) of the ICBM is 1000 lb/ft^2 or 0.002 $m^3/kgsec^2$ according to different definitions.

The spherical portion of the glass shield at the stagnation point is assumed to have a diameter of 0.635 m.

MATERIAL PROPERTIES AND FUNCTIONS EMPLOYED

Since there is a lack of experimental data at high temperatures for the thermal conductivity (k), the specific heat (c_p), and the emissivity constant (ϵ), these material properties were treated as non-temperature-dependent constants for each calculated glass shield. The effect of the variation of these material property constants is, however, investigated by the calculation of 26 supposedly opaque glass shields (see Table 1) with each glass shield having a different set of material properties. The specific weight (γ) is assumed to be 2105 kg/m^3 for all the calculated glass shields in this report.

Since experimental data is available for the viscosity and the vapor pressure as a function of the temperature, these two material properties of glass were treated as temperature-dependent functions for each calculated glass shield. The viscosity functions for Pyrex (Corning 7900) and fused silica (quartz) are curve fits of curves presented in Figure 9 of reference 11. The vapor pressure function and heat of vaporization (h_v) for Pyrex were taken from reference 7. The vapor pressure function and heat of vaporization for fused silica were taken from reference 9. When the constants μ^* and A in the viscosity and vapor pressure functions are equal to one, the equations given below for μ and p_v are the exact curve fits of these two properties for Pyrex and fused silica glasses.

The vapor pressure function, viscosity function, and heat of vaporization for Pyrex and fused silica glass are as follows:

(1) Pyrex glass

(a) the vapor pressure function

$$p_{v,P} = 10{,}332\ A_P \exp\left[\frac{-46{,}400}{T(^\circ K)} + 14.5\right] \quad (kg/m^2) \tag{1}$$

(b) the viscosity function

$$\mu_P = 0.016684\ \mu^*_P \exp\left[\left(\frac{4230}{T(^\circ K)}\right)^{2.0635}\right] \quad (kg\ sec/m^2) \tag{2}$$

(c) the heat of vaporization

$$h_{v,P} = 2470\ (kcal/kg)$$

(2) Fused silica (quartz)

(a) the vapor pressure function

$$p_{v,F.S.} = 10{,}332 \exp\left[\frac{-57{,}800}{T(^\circ K)} + 18.48\right] \quad (kg/m^2) \tag{3}$$

(b) the viscosity function

$$\mu_{F.S.} = 4.9505 \exp\left[\left(\frac{4836.97}{T(°K)}\right)^{2.6366}\right] \quad (kg\ sec/m^2) \qquad (4)$$

(c) the heat of vaporization

$$h_{v,F.S.} = 3050\ (kcal/kg)$$

The constants μ_P^* and A_P are one for the real material and were varied in some of the cases studied here.

The material properties that were varied and the limits within which each material property is varied in this report are as follows:

(1) the thermal conductivity, k (kcal/m °K sec)

$$0.61 \times 10^{-4} \leq k \leq 48.84 \times 10^{-4}$$

(2) the specific heat, c_p (kcal/kg °K)

$$0.10 \leq c_p \leq 0.58$$

(3) the emissivity constant, ϵ (-)

$$0.40 \leq \epsilon \leq 1.0$$

(4) the viscosity level, μ_P^* (-)

$$0.10 < \mu_P^* < \infty$$

(5) the vapor pressure level A_P

$$0 \leq A_P \leq 1000$$

Since the cases as the individual material properties k, c_p, and μ^* approach zero and infinity were discussed in reference 1, they will not be repeated in this report.

A so-called "standard set" of material properties will be referred to in this report, and they are as follows:

$k = 0.61 \times 10^{-4}$ (kcal/m°K sec)

$c_p = 0.29$ (kcal/kg °K)

$\epsilon = 0.8$ (-)

$\mu_p^* = 1.0$ (-)

$A_p = 0$ (-)

The "standard set" of material properties was employed in the theoretical study of the ablation of a glass shield at the stagnation point of a re-entering IRBM [1] and a re-entering satellite [6].

THE EFFECT OF THE MATERIAL PROPERTIES ON THE INTERFACE TEMPERATURE

The interface temperature T_i follows the same trend with respect to time for each glass shield regardless of the material properties, and the maximum interface temperature occurs at approximately the same time for each shield since $h_e \gg h_i$. Therefore, the effect of the material properties on the interface temperature can be studied by the consideration of the maximum interface temperature ($T_{i,max}$) for the ICBM re-entry. Figure 3 shows the effect of the material properties on the maximum interface temperature. Large values for the thermal conductivity k, specific heat c_p, emissivity constant ϵ, and vapor pressure level A tend to keep the surface temperature low; the viscosity level μ^* has very little effect on the surface temperature.

Figure 4 is a pictorial view of a Pyrex glass shield (Case 24, Table 1) showing its complete temperature and ablation history for the ICBM re-entry. One can see the movement of the interface at the melting rate $-v_{oo}$(mm/sec) toward the thermally insulated inner edge of the glass shield in this graph.

THE HEAT FLUXES

1. The Aerodynamic Heat Flux

The compression at and near the forward surface and the friction between the fluid particles as they flow along the body converts the kinetic energy of motion into aerodynamic heat. The formulas that were used for the aerodynamic heat flux rate at the stagnation point of a non-ablating surface and the source of these formulas are as follows:

(1) Molecular flow region [10]

$$\bar{q}_{aero} = 1.054 \times 10^{-3} \rho_\infty V_{oo} \left[V_{oo}^2 - 1.9263 \times 10^3 (T_i - T_{oo}) \right] \text{ kcal/m}^2\text{sec} \qquad (5)$$

(2) Continuum flow region for $V_{oo} \geq 2100$ m/sec [8]

$$\bar{q}_{aero} = 74{,}571.6 \sqrt{\rho_\infty / R}\ (V_{oo}/u_c)^{3.15} \left(\frac{h_e - h_i}{h_e - 73}\right) \text{ kcal/m}^2\text{sec} \tag{6}$$

(3) For $V_{oo} < 2100$ m/sec [12]

$$\bar{q}_{aero} = (k\sqrt{\mu})_{i,air}\ (T_e - T_i) \sqrt{T_e \rho_e / T_i}\ (Nu \sqrt{Re_i})_{Pr\,=\,1}\ (.715)^{0.4}\ \sqrt{K_M \cdot V_\infty / D}$$

$$\text{kcal/m}^2\text{sec.} \tag{7}$$

The aerodynamic heat flux for an ablating surface, e.g., glass vaporization, is given by

$$q_{aero} = \bar{q}_{aero}\ \psi \tag{8}$$

where ψ is given in Reference 7 as

$$\psi = \frac{1 - c}{1 - (1 - K_1 M^{n_1})c} \tag{9}$$

$$c = \frac{1}{1 + M\left(\frac{p_e}{p_v} - 1\right)} . \tag{10}$$

For the glass shields considered herein, $M = 0.72$, $K_1 = 0.68$, and $n_1 = 0.26$. The relation for the surface ablation taken from reference 7 is

$$(\gamma v)_i = \frac{-\bar{q}_{aero}\ c}{(h_e - h_i)\ [1 - (1 - K_1 M^{n_1})c]} . \tag{11}$$

The time $t = t^*$(sec) designates the time after ablation has ended when the net heat flux

$$q_i = q_{aero} - q_{rad} + h_v(\gamma v)_i \tag{12}$$

across the surface changes its sign from positive to negative. Beginning then, the radiative heat transfer q_{rad} out of the shield exceeds the aerodynamic heating

rate q_{aero}. The time t^* is between the time of peak heating and impact time and is approximately the same for all the glass shields. All of the individual heat fluxes for each glass shield were integrated over time t to $t = t^*$, since

$$Q_i(t^*) = \int_0^{t^*} q_i \, dt$$

gives the maximum amount of heat that the shield, in both the solid and the liquid stage, will absorb. The time integrated q's to t^* will be designated $Q(t^*)$ in this report.

The aerodynamic heat flux $\bar{Q}_{aero}(t^*)$ that stands for the time integrated aerodynamic heat flux without mass flow across the interface is given for each one of the calculated glass shields in Table 1. The true aerodynamic heat flux, $Q_{aero}(t^*)$, is given by

$$Q_{aero}(t^*) = \bar{Q}_{aero}(t^*) - Q_{Bl} + \int_0^{t^*} h_v \, (-\gamma v)_i \, dt, \tag{13}$$

where $Q_{Bl}(t^*)$ is the total amount of aerodynamic heat blocked up to time t^* due to the vaporization process of the glass. Table 1 shows that the total aerodynamic heat, $\bar{Q}_{aero}(t^*)$, changes very little for all of the calculated cases since $h_e \gg h_i$ during the period of significant heating. Thus, the material properties of the glass shield have very little effect on the aerodynamic heat flux $\bar{Q}_{aero}$. The trajectory of the re-entering vehicle principally determines the aerodynamic heat flux $\bar{Q}_{aero}$.

2. The Heat Flux Radiated Away From the Opaque Glass Shields

The heat flux that is radiated away from the outer surface of the supposedly opaque glass shield given by

$$q_{rad} = 1.378 \times 10^{-11} \, \epsilon \, T_i^4 \quad (kcal/m^2 \, sec) \tag{14}$$

is a function of the wall temperature and emissivity constant ϵ. The values of $Q_{rad}(t^*)$ listed in Table 1 show that the outer surface radiates away the major portion of the aerodynamic heat flux $\bar{Q}_{aero}(t^*)$ for most of the calculated shields. The radiative efficiency of the glass shields is defined as the fraction $Q_{rad}(t^*)/\bar{Q}_{aero}(t^*)$ of the gross heat input that is radiated away from the glass wall. Figure 5 shows the radiative efficiency of the heat protection shields for the varied material properties assumed for the glass. This graph shows that the radiative efficiency of a glass heat shield is optimized by utilizing a glass with a small thermal conductivity and specific heat and with a small vapor pressure Changes in the viscosity level and emissivity constant have a much smaller effect on the radiative efficiency than the other pertinent material problems.

3. The Heat Blocked, $Q_{Bl}(t^*)$, Due to the Vaporization Process of the Glass

The total amount of heat blocked due to the vaporization is given by

$$Q_{Bl} = \bar{Q}_{aero} - Q_{aero} + h_v \int_o^{t^*} (-\gamma v)_i \, dt, \tag{15}$$

where $(\bar{Q}_{aero} - Q_{aero})$ represents the amount of heat blocked by the diffusion of the vapor across the boundary layer and

$$h_v \int_o^{t^*} (-\gamma v)_i \, dt$$

is the amount of heat absorbed by the evaporation process at the surface of the shield. Cases calculated for A_p = 1, 3, 100, and 1000 (Table 1), with all other material properties being the so-called "standard set" of material properties, resulted in 46 to 88 percent of the total aerodynamic heat $\bar{Q}_{aero}(t^*)$ being blocked. The amount of the total ablation that was due to vaporization ranged from 53 to 98 percent. Reference 5 points out that radiative cooling is more desirable than mass transfer cooling under certain conditions.

4. The Heat Flux $Q_i(t^*)$ Absorbed by the Glass Shield

The total amount of heat that the molten and solid layers of the shield absorb is given by

$$\begin{aligned} Q_i(t^*) &= \bar{Q}_{aero}(t^*) - Q_{rad}(t^*) - Q_{Bl}(t^*) = \\ &= Q_{aero}(t^*) - Q_{rad}(t^*) - h_v \int_o^{t^*} (-\gamma v)_i \, dt. \end{aligned} \tag{16}$$

This total heat absorbed $Q_i(t^*)$ per unit area by the shield ranges from 3146 kcal/m^2 to 60,000 kcal/m^2 for all cases calculated. The amount of the total aerodynamic heat $\bar{Q}_{aero}(t^*)$ absorbed by the shield ranged from 7 to 91 percent.

Figure 6, presenting $Q_i(t^*)$ as a function of the material properties, shows that the thermal conductivity and specific heat affect the magnitude of absorbed heat $Q_i(t^*)$ by the shield much more than the other material properties. The amount of heat $Q_i(t^*)$ should be small since then the shield thickness needed as a heat sink is kept to a minimum. $Q_i(t^*)$ can be kept small by employing a glass with a small thermal conductivity, a small specific heat, a high viscosity and vapor pressure level, and a large emissivity at the surface.

5. The Amount $Q_c(t^*)$ of the Absorbed Heat Carried Away by the Molten Flow

The convective heat flux $Q_c(t^*)$ is the amount of heat that the flow of molten glass carries away from the stagnation point vicinity. This heat $Q_c(t^*)$ carried away by the liquid glass is part of the heat $Q_i(t^*)$ that was absorbed by the glass shield. Table 1 shows that from 0 to 79 percent of the total aerodynamic heat $\bar{Q}_{aero}(t^*)$ is carried away by the molten flow. The amount of the heat absorbed $Q_i(t^*)$ that is carried away by the molten flow ranged from 0 to 96 percent. Table 1 and Figure 6 show that those shields which absorbed a large percentage of the total heat $\bar{Q}_{aero}(t^*)$ had most of this absorbed heat $Q_i(t^*)$ carried away by the molten flow.

The difference $Q_i(t^*) - Q_c(t^*)$ is that amount of heat the glass shield will have to store in heat sink fashion at the stagnation point, because after time t^* no more convective cooling takes place since melting has stopped. After time t^* the heat $Q_i(t^*) - Q_c(t^*)$ is very important since this heat keeps penetrating into the shield until impact time t_f. The fraction $R(t^*)$ given by $(Q_i(t^*) - Q_c(t^*))/\bar{Q}_{aero}(t^*)$ is the fraction of the gross heat $\bar{Q}_{aero}(t^*)$ that is stored in heat sink fashion in the shield. This fraction $R(t^*)$ varies from 0.027 to 0.122; this shows that the glass shields have to store very little of the gross heat.

THE ABLATION OF THE GLASS SHIELDS

The ablation rate, $-v_{oo}$ (mm/sec), of the glass shield is due to (1) the flow of molten glass and (2) the evaporation of the glass at the surface. The total ablation s, i.e., the layer lost due to ablation, given by

$$s = \int_0^{t_f} -v_{oo}\, dt \qquad (17)$$

for each glass shield, is given in Table 1. For the shields investigated, the thickness s of the heat shield lost due to ablation was from 0 to 35 mm, amounting to less than 1.4 inches.

Figure 7 shows the total ablation s as a function of the material properties of the glass shield. Figures 7, 8, and 9 show that the thermal conductivity k, and the specific heat c_p are the material properties that principally determine the total ablation s when the ratio $k/\gamma c_p$ is small, as is desirable. Practical variations of the viscosity level μ^*, surface emissivity ϵ, and the vapor pressure level A caused rather small variations in the total ablation for the glass shields which had a small thermal diffusivity $k/\gamma c_p$.

The dependency of s on the viscosity level for a non-vaporizing glass shield is shown in Figure 8 by comparison of s for cases 8, 19, and 20. All three cases have the properties $k = 9.7 \times 10^{-4}$ kcal/m °K sec, $c_p = 0.29$ kcal/kg °K,

$k/\gamma c_p = 15.9 \times 10^{-7}$ m^2/sec, and $A_p = 0$. The viscosity level μ^*_p was varied within the limits $0.1012 \leq \mu^*_p \leq 101.2$ which resulted in the total ablation s ranging between $9.3 \leq s \leq 35.7$ mm. Evidently, s increases with a decreasing viscosity level.

The effect of varying k and c_p for a large constant ratio $k/\gamma c_p$ is shown by comparing Cases 21 and 22 (Fig. 8) where $k/\gamma c_p = 40 \times 10^{-7}$ m^2/sec for both cases; Case 21 has values of k and c_p which are smaller than those of Case 22 by a factor of two. Case 21 with the smaller k and c_p resulted in an ablated layer 59% larger than that of Case 22.

Cases 2, 10, 11, 25, and 26 in Table 1 and Figure 7 show the effect on the total ablation s of varying the vapor pressure level A_p between the limits $0 \leq A_p \leq 1000$. The total ablation s increases only slightly with increasing vapor pressure level. Table 1 shows that the fraction

$$\left(\int_0^{t_f} - v_i \, dt\right) \Big/ s$$

of the total ablation due to vaporization is as large as 98% for $A_p = 1000$, and that this fraction increases together with the vapor pressure level A and viscosity level μ^*.

THE THERMAL PENETRATION INTO THE GLASS SHIELD

The calculated "semi-infinite solution" [3] is based on the condition that

$$\lim_{z \to \infty} T(t, z) = T_o$$

where T_o was assumed to be 300°K in this report. For all the cases considered, a thermally insulated inner wall of the shield was assumed to have been placed at the maximum distance (denoted $z = b$) from the final surface where the semi-infinite solution yielded T = 380°K. For the given re-entry, the time of maximum thermal penetration was impact time t_f. The true temperature at the point b and time t_f is

$$T(t_f, b) = T_o + 2(380 - T_o) = 460°K, \tag{18}$$

which follows from adding the temperature profile given by the semi-infinite solution to the reflection of this profile about the point b. This satisfies the conditions that $\partial T(t_f, b)/\partial z = 0$ and that the temperature of the thermally insulated inner wall is $\leq 460°K$. The numerical results show that this assumption causes a negligible temperature increase at the outer surface.

The maximum thermal penetration b, or the thickness of glass needed as a heat sink, is given in Table 1 for all of the calculated cases and is plotted as a function of the material properties in Figure 7. The thickness b varies from 2.6 to 21.15 mm (Table 1). Figure 7 shows that the thermal penetration b is predominantly governed by the thermal conductivity k and specific heat c_p. The viscosity level μ^* has some effect on b, but not as much as k or c_p, whereas the emissivity ϵ of the surface and the vapor pressure level A had an almost negligible effect on this thickness b (Fig. 7 and 8) since large percentages of the total radiation emitted from the surface and the total transport of material by melt flow and evaporation are concentrated in the short-lasting, high-temperature range of the surface. In this range, small changes in the surface temperature can compensate for large changes in the emissivity constant and in the assumed level factors A and μ^* of the vapor pressure and viscosity, respectively, because of the highly nonlinear relations $p_v = p_v(T)$, $\mu = \mu(T)$, and $q_{rad} = q_{rad}(T)$.

Figure 8 shows the thermal penetration b as a function of the thermal diffusivity $k/\gamma c_p$ for all the calculated glass shields; it is seen that b increases together with $k/\gamma c_p$ and μ^*

THE NECESSARY WEIGHT OF THE GLASS SHIELDS

The necessary weight per unit area of the glass shield, defined as $\gamma(s + b)$, is the most important parameter of the ablation type heat shield to be considered; the sum (s + b) is defined as the necessary thickness. The weight of the protective glass shield should be kept as light as possible, but the shield should still successfully protect the re-entry body. The specific weight γ of the glass shields was assumed to be constant, i.e., $\gamma = 2105$ kg/m^3, in this report; therefore, the two constituents that determine the necessary weight $\gamma(s + b)$ are the total ablation s and the heat sink thickness b.

For an IRBM re-entry [4], the thermal diffusivity $k/\gamma c_p$ was the dominant material parameter that determined the necessary thickness (s + b) of a glass shield in the vicinity of the stagnation point. Melting and significant aerodynamic heating stopped about 40 seconds before impact time for the IRBM re-entry. Since s was considerably smaller than b, the dependency of (s + b) on the material properties other than $k/\gamma c_p$ was small.

For the ICBM re-entry at hand, melting and significant aerodynamic heating stopped only 15 seconds before impact time; also, the contribution of the total ablation s to the necessary thickness (s + b) is quite significant except for the cases where the viscosity level was assumed to be so high that little melting occurred. Therefore, (s + b) is affected by other parameters in addition to $k/\gamma c_p$. Figure 9 presents the necessary weight as a function of the thermal diffusivity $k/\gamma c_p$ for all the glass shields calculated. From the results it is concluded that the following trend in the material properties would provide the lightest glass heat protection shield for the ICBM re-entry:

(1) a small thermal diffusivity $k/\gamma c_p$,
(2) a high viscosity level, i.e., a large resistance to melting,
(3) a large emissivity ϵ of the supposedly opaque glass.

The results show that the vapor pressure level A has a negligible effect on the necessary weight γ (s + b).

CONCLUSIONS

The heat protection at the stagnation point of an ICBM re-entering the atmosphere of the earth is investigated in this report by using homogeneous, opaque glass shields. The effect of the material properties of the glass on the performance parameters is analyzed from the results of 26 calculated glass shields, each with a different set of assumed material properties.

The most important performance parameter of the heat protection device is the necessary weight γ (s + b) per unit area that is needed to keep the thermally insulated inner edge of the shield below an arbitrarily chosen low temperature of 460°K. The following trends of the glass thermal properties would tend to minimize the weight of the glass heat protection shield for the ICBM re-entry:

(1) a small thermal diffusivity $k/\gamma c_p$,
(2) a high viscosity level, i.e., a large resistance to melting,
(3) a large emissivity constant ϵ of the supposedly opaque glass; this is not as important as the thermal diffusivity or the viscosity of the glass.

It was found that the vaporization of the glass had very little effect on the necessary weight γ (s + b).

TABLE 1. THE CALCULATED GLASS SHIELDS FOR THE ICBM

Case No.	$k \times 10^6$	c_p	$\frac{k}{\gamma c_p} \times 10^7$	μ^*	ϵ	A	t^*	$\bar{Q}_{aero}(t^*)$	$Q_{Bl}(t^*)$	$Q_{rad}(t^*)$	$Q_l(t^*)$	$Q_c(t^*)$	$T_{l,max}$	$\frac{Q_{Bl}(t^*)}{\bar{Q}_{aero}(t^*)}$	$\frac{Q_{rad}(t^*)}{\bar{Q}_{aero}(t^*)}$	$\frac{Q_l(t^*)}{\bar{Q}_{aero}(t^*)}$	$\frac{Q_c(t^*)}{Q_l(t^*)}$	$\int_0^{t^*} -v_l\,dt$	a	$\frac{\int_0^{t^*} -v_l\,dt}{a}$	$k_w \gamma \int_0^{t^*} -v_l\,dt$	$\frac{k_w \gamma \int_0^{t^*} -v_l\,dt}{Q_{Bl}}$	b	a + b	$\gamma(a+b)$
	$\frac{kcal}{m\,°K\,sec}$	$\frac{kcal}{kg\,°K}$	$\frac{m^2}{sec}$				sec	$\frac{kcal}{m^2}$	$\frac{kcal}{m^2}$	$\frac{kcal}{m^2}$	$\frac{kcal}{m^2}$	$\frac{kcal}{m^2}$	°K					mm	nhm		$\frac{kcal}{m^2}$		mm	mm	$\frac{kg}{m^2}$
1	.61	.10	2.8979	1.0 (P)	.8	0	53.65	56,414	0	49,292	7,122	6,487	4,580	0	.874	.126	.911	0	10.41	0	0	0	5.29	16.33	34.375
2	.61	.29	.99926	1.0 (P)	.8	0	53.35	56,628	0	47,094	9,534	8,695	4,539	0	.832	.168	.912	0	4.77	0	0	0	3.48	8.25	17.366
3	.61	.58	.49963	1.0 (P)	.8	0	53.10	56,813	0	45,147	11,666	10,226	4,505	0	.795	.205	.876	0	2.79	0	0	0	2.60	5.39	11.346
4	5.00	.10	23.753	1.0 (P)	.8	0	54.55	58,781	0	34,056	24,725	23,481	4,156	0	.579	.421	.950	0	41.34	0	0	0	15.37	56.71	119.370
5	5.00	.29	8.1907	1.0 (P)	.8	0	54.40	59,444	0	29,001	30,443	28,389	4,003	0	.488	.512	.933	0	17.42	0	0	0	9.27	26.69	56.187
6	5.00	.58	4.095	1.0 (P)	.8	0	54.20	60,078	0	25,562	34,516	31,387	3,901	0	.425	.575	.909	0	9.77	0	0	0	6.80	16.56	34.861
7	9.713	.10	46.143	1.0 (P)	.8	0	54.80	60,123	0	26,492	33,631	31,965	3,882	0	.441	.559	.950	0	59.67	0	0	0	21.08	80.75	169.980
8	9.713	.29	15.911	1.0 (P)	.8	0	54.65	61,125	0	21,405	39,720	36,999	3,691	0	.350	.650	.931	0	24.36	0	0	0	12.80	37.16	78.222
9	9.713	.58	7.956	1.0 (P)	.8	0	54.60	61,881	0	18,132	43,749	39,314	3,572	0	.293	.707	.899	0	13.16	0	0	0	9.69	22.85	48.099
10	.61	.29	.99926	1.0 (P)	.8	1 (P)	53.35	58,979	26,811	27,841	4,327	3,590	3,805	.455	.472	.0734	.830	2.493	4.75	.525	12,962	.483	3.44	8.18	17.227
11	.61	.29	.99926	1.0 (P)	.8	3 (P)	53.40	59,949	34,258	22,553	3,146	2,369	3,542	.571	.376	.0525	.753	3.194	4.78	.669	16,607	.485	3.44	8.21	17.286
12	.61	.29	.99926	∞ (P)	.8	0	47.20	50,650	0	47,104	3,546	0	4,679	0	.930	.0700	0	0	0	0	0	0	6.76	6.76	14.230
13	.61	.29	.99926	374.61 (P)	.8	0	48.90	54,184	0	50,207	3,977	1,307	4,672	0	.927	.0734	.329	0	.77	0	0	0	5.71	6.48	13.660
14	.61	.29	.99926	100.0 (P)	.8	0	50.30	55,473	0	51,023	4,450	2,430	4,661	0	.920	.0802	.546	0	1.30	0	0	0	5.15	6.45	13.577
15	.61	.29	.99926	.3746 (P)	.8	0	53.75	56,920	0	45,146	11,774	11,115	4,486	0	.793	.207	.944	0	6.09	0	0	0	3.36	9.45	19.892
16	.61	.29	.99926	.10 (P)	.8	0	54.25	57,473	0	41,633	15,840	15,152	4,383	0	.724	.276	.957	0	8.57	0	0	0	3.15	11.72	24.671
17	.61	.29	.99926	1.0 (P)	.4	0	53.62	53,489	0	40,759	12,730	11,925	5,211	0	.762	.238	.937	0	5.83	0	0	0	3.44	9.27	19.513
18	.61	.29	.99926	1.0 (P)	1.0	0	53.20	57,610	0	48,993	8,616	7,764	4,335	0	.850	.150	.901	0	4.42	0	0	0	3.46	7.88	16.596
19	9.713	.29	15.911	.1012 (P)	.8	0	55.34	63,450	0	13,500	49,950	47,537	3,208	0	.213	.787	.952	0	35.65	0	0	0	12.09	47.74	100.488
20	9.713	.29	15.911	101.198 (P)	.8	0	52.60	57,831	0	36,549	21,281	16,577	4,349	0	.632	.368	.779	0	9.25	0	0	0	16.32	25.57	53.825
21	24.418	.29	40.00	1.0 (P)	.8	0	55.21	63,450	0	12,261	51,228	47,149	3,181	0	.193	.807	.743	0	35.32	0	0	0	20.04	55.36	116.530
22	48.836	.58	40.00	1.0 (P)	.8	0	55.40	65,930	0	5,954	59,948	51,892	2,686	0	.0903	.909	.787	0	22.18	0	0	0	21.15	43.33	91.210
23	5.00	.29	8.1907	1.0 (F.S.)	.8	1 (F.S.)	50.42	58,799	31,592	21,009	6,198	342	3,592	.537	.357	.105	.0552	2.555	2.74	.932	16,404	.519	15.43	18.17	38.244
24	5.00	.29	8.1907	1.0 (P)	.8	1 (P)	54.45	60,539	15,124	21,514	23,901	21,946	3,643	.250	.355	.395	.918	1.389	15.97	.087	7,222	.478	9.25	25.22	53.090
25	.61	.29	.99926	1.0 (P)	.8	100 (P)	53.70	65,480	52,850	11,463	1,167	395	2,838	.807	.175	.018	.338	4.930	5.26	.937	25,633	.485	3.23	8.49	17.871
26	.61	.29	.99926	1.0 (P)	.8	1000 (P)	53.90	67,214	58,853	7,516	844	112	2,495	.876	.112	.013	.133	5.470	5.58	.980	28,440	.483	3.17	8.75	18.419

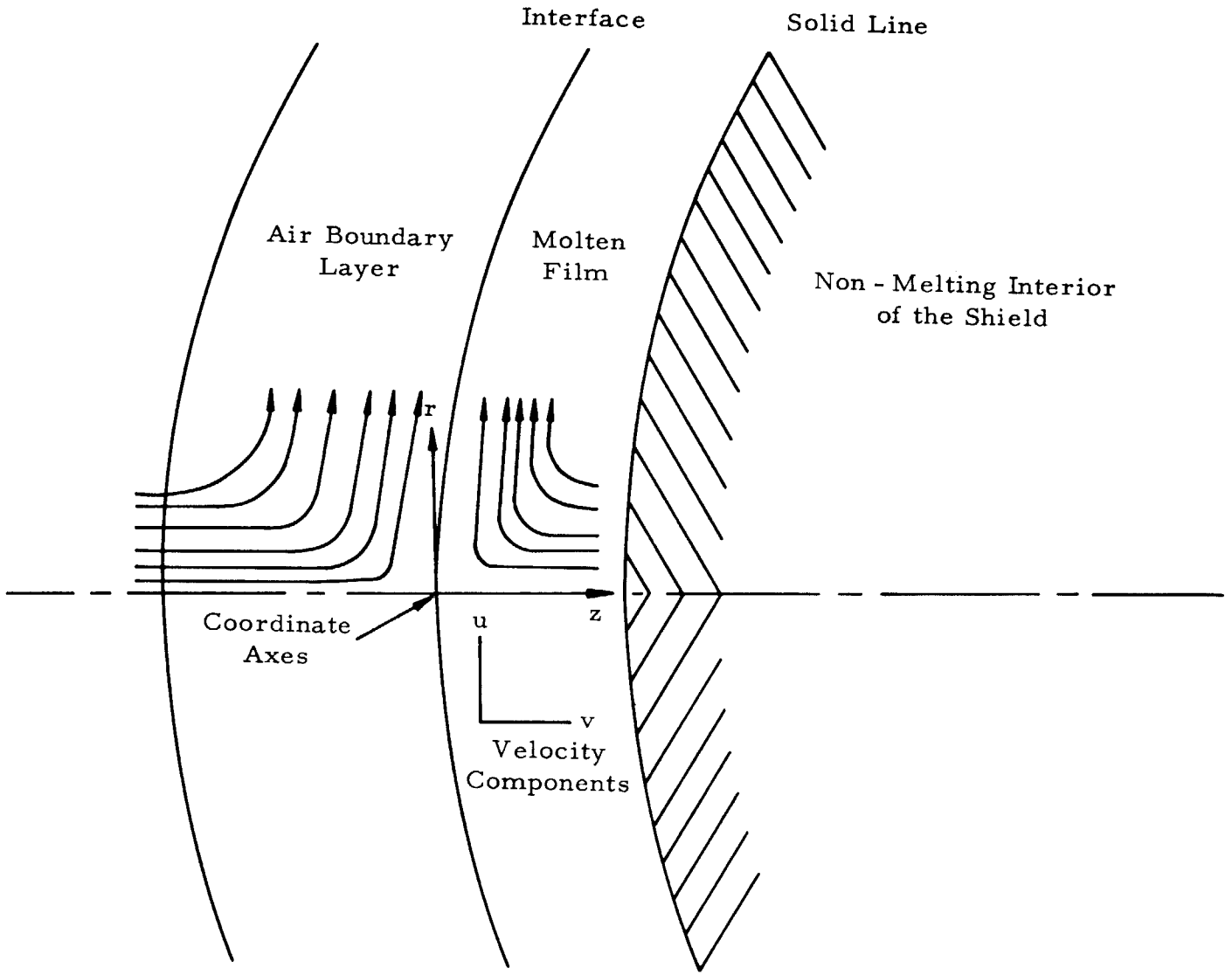

FIG. 1. THE REFERENCE SYSTEM

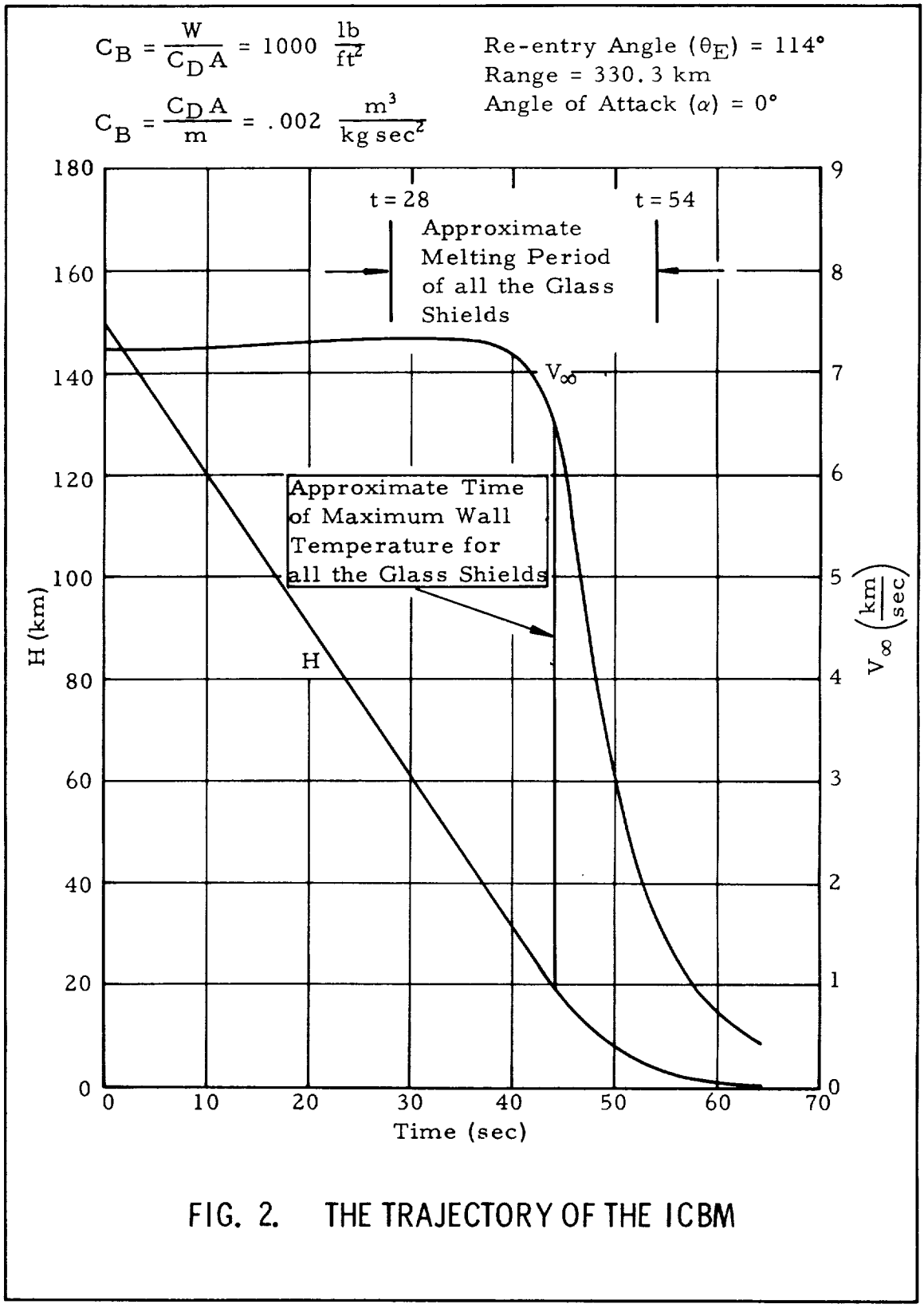

FIG. 2. THE TRAJECTORY OF THE ICBM

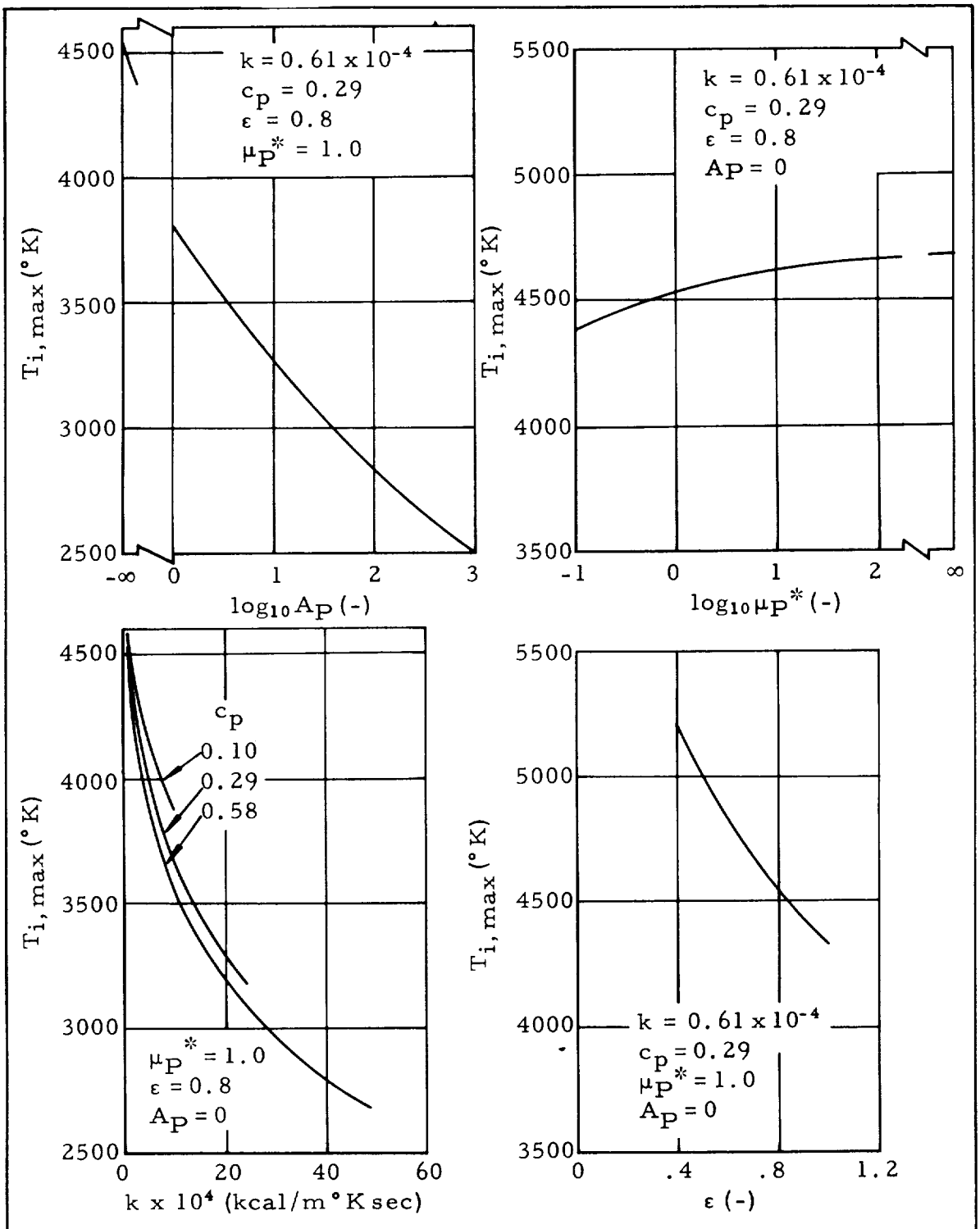

FIG. 3. THE MAXIMUM INTERFACE TEMPERATURE AS A FUNCTION OF THE MATERIAL PROPERTIES

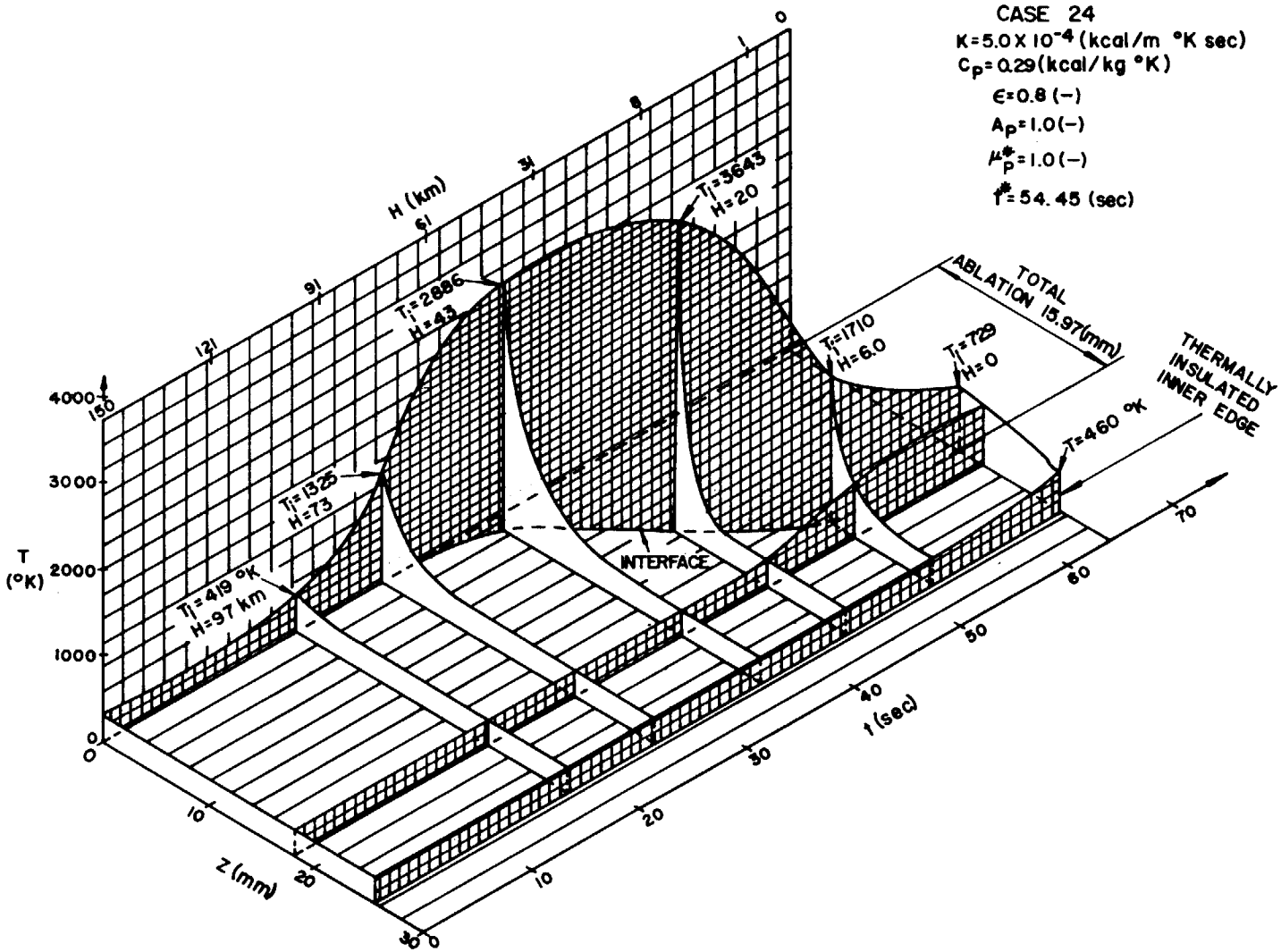

FIG. 4. TEMPERATURE AND ABLATION HISTORY OF A GLASS SHIELD AS A FUNCTION OF THE MATERIAL PROPERTIES

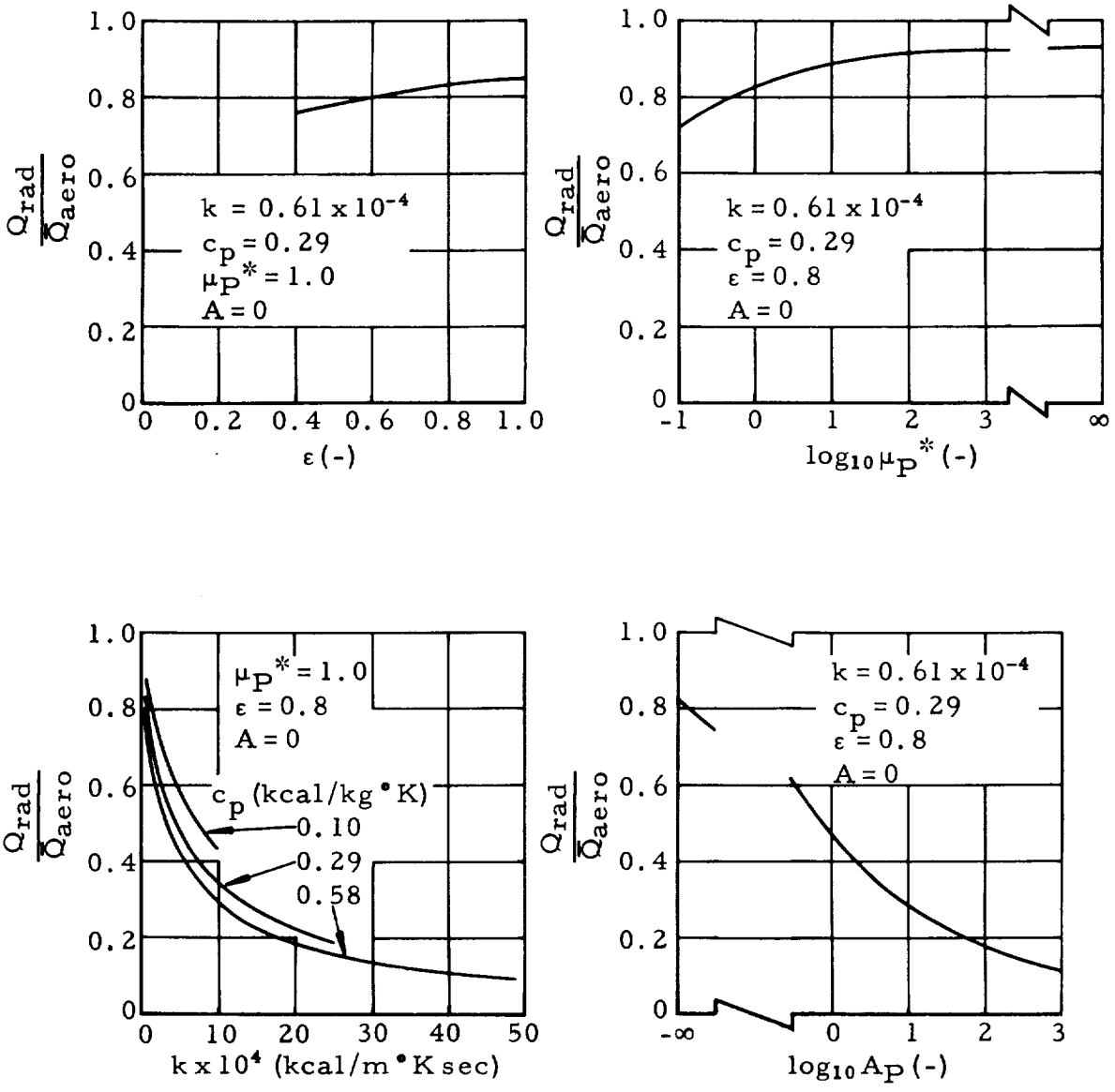

FIG. 5. THE RADIATIVE EFFICIENCY OF THE GLASS SHIELDS AS A FUNCTION OF THE MATERIAL PROPERTIES

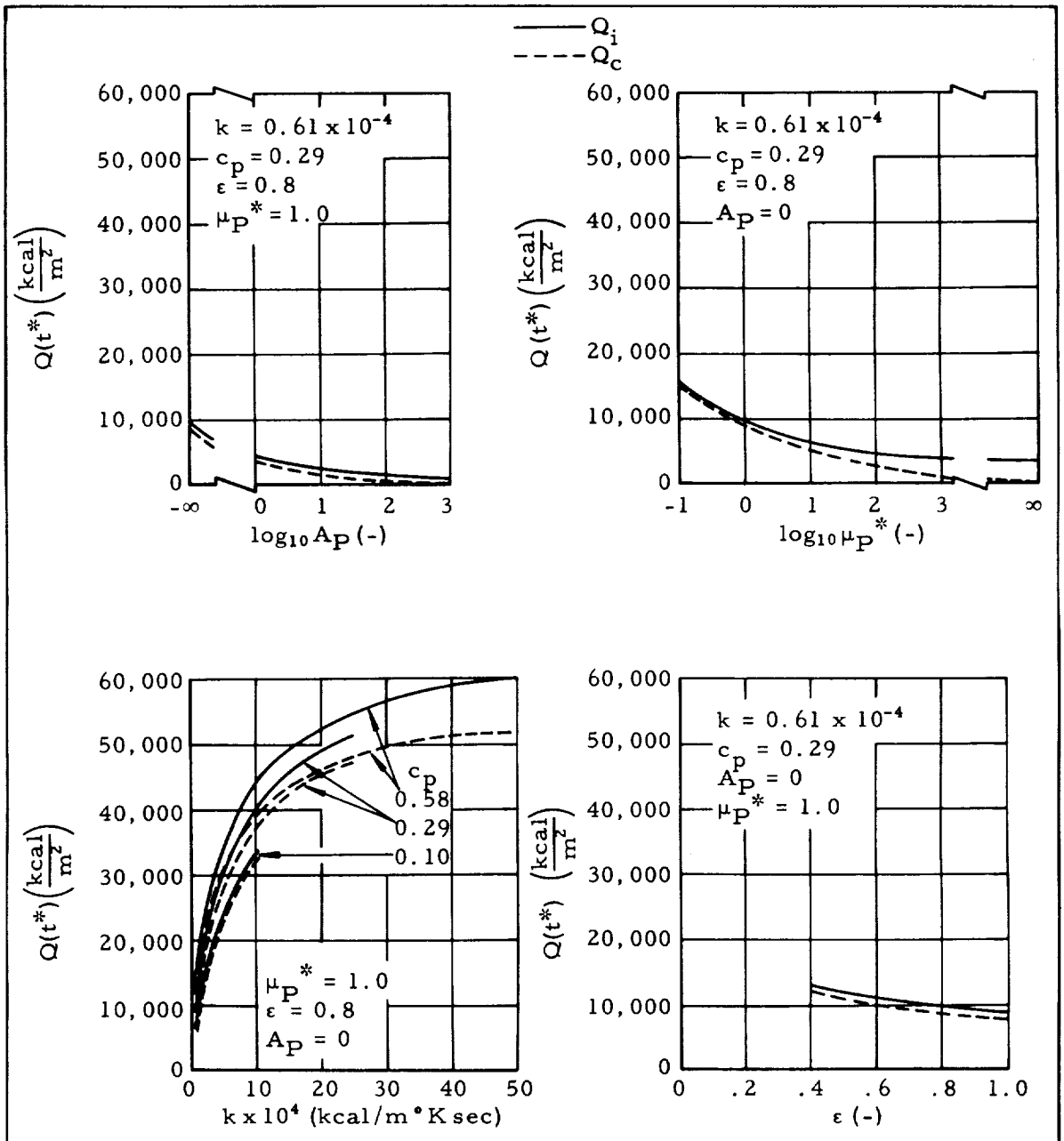

FIG. 6. THE HEAT ABSORBED $Q_i(t^*)$ BY THE GLASS SHIELDS AND THE AMOUNT $Q_C(t^*)$ OF THE ABSORBED HEAT THAT IS CARRIED AWAY BY THE FLOW OF THE LIQUID GLASS AS A FUNCTION OF THE MATERIAL PROPERTIES

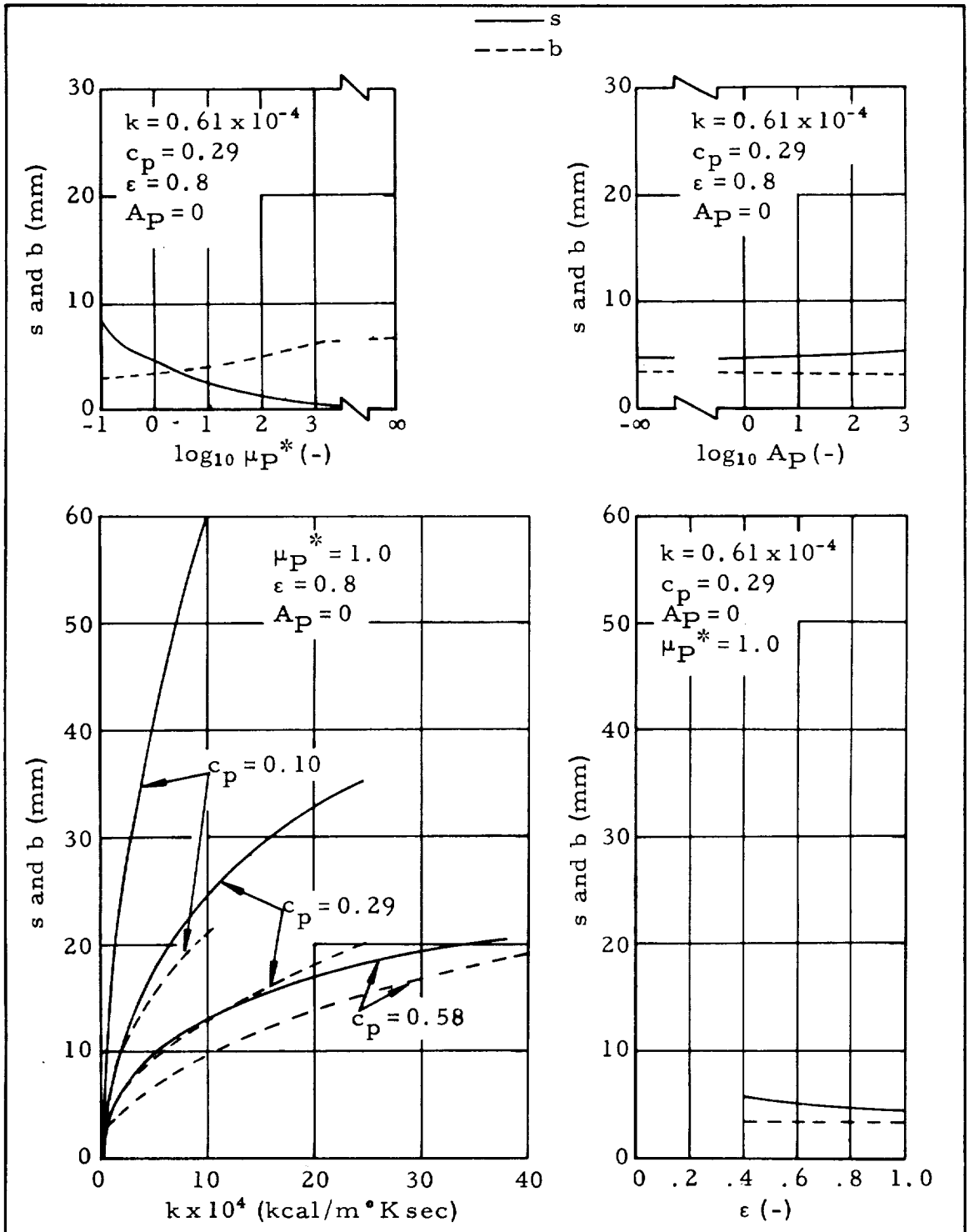

FIG. 7. THE TOTAL ABLATION s and THERMAL PENETRATION b AS A FUNCTION OF THE MATERIAL PROPERTIES

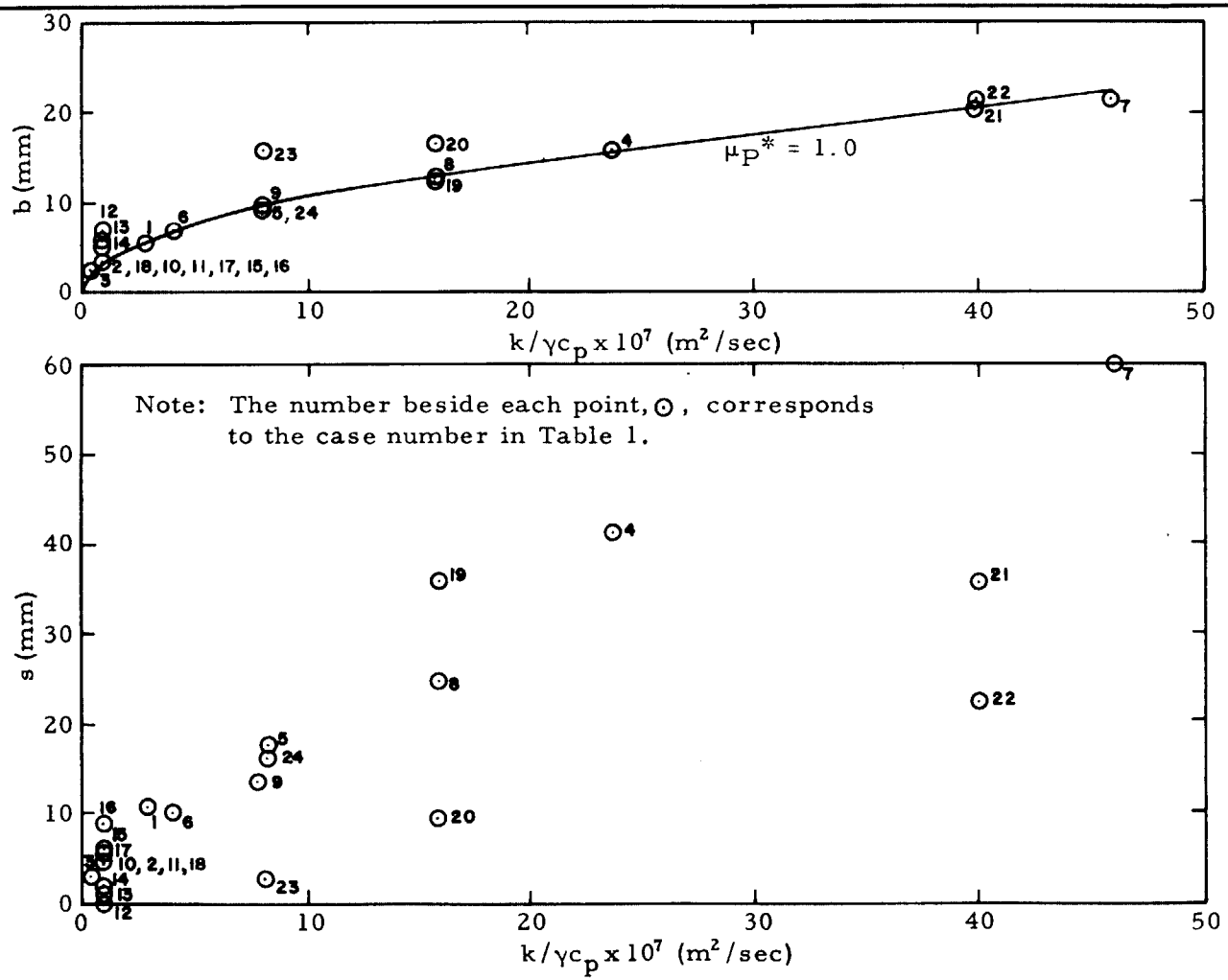

FIG. 8. THE TOTAL ABLATION s AND THERMAL PENETRATION b AS A FUNCTION OF THE THERMAL DIFFUSIVITY $k/\gamma c_p$ FOR ALL THE CALCULATED GLASS SHIELDS

REFERENCES

1. Adams, E. W., "Theoretical Investigations of the Ablation of a Glass-type Heat Protection Shield of Varied Material Properties at the Stagnation Point of a Re-entering IRBM," NASA TN D-564, January 1961.

2. Adams, E. W., "Radiation Versus Mass Transfer Effects for Ablation Re-entry Shields of a Nonlifting Satellite," Journal of the Aero/Space Sciences, Readers Forum, Vol. 27, No. 11, November 1960.

3. Adams, E. W., "Calculation Method for the Transient Melting Process of a Glassy Heat Protection Shield in the Vicinity of the Stagnation Point of a Re-entering Vehicle," ABMA Report DA-TR-8-60, March 1960.

4. Adams, E. W., "The Thickness of a Melting Ablation Type Heat Shield," Journal of the Aero/Space Sciences, Readers Forum, Vol. 27, No. 7, July 1960

5. Adams, E. W., "Analysis of Quartz and Teflon Shields for a Particular Re-entry Mission," Proceedings of the 1961 Heat Transfer and Fluid Mechanics Institute, Stanford University Press, 1961, pp. 222-236.

6. Adams, E. W., "Melting-Type Heat Protection of a Ballistic Satellite Re-entering the Atmosphere of the Earth," Fusees et Recherche Astronautique et Spatiale, Paris, pp. 7-20.

7. Bethe, H. A., and Adams, M. C., "A Theory for the Ablation of Glassy Materials," Journal of the Aero/Space Sciences, Vol. 26, June 1959, pp. 321-328.

8. Detra, R. W., Kemp, N. H., and Riddell, F. R., "Addendum to Heat Transfer to Satellite Vehicles Re-entering the Atmosphere," Jet Propulsion, pp. 1256-1257, December 1957.

9. Georgiev, S., "Unsteady Ablation," Semi-Annual Report on the Re-entry Problem, AVCO Corporation, December 1958.

10. Oppenheim, A. K., "Generalized Theory of Convective Heat Transfer in a Free Molecular Flow," Journal of the Aero/Space Sciences, Vol. 21, July 1954, pp. 459-474.

11. "Properties of Selected Commercial Glasses," Corning Glass Works, Corning, New York, 1959.

12. Reshotko, E., and Cohen, C. B., "Heat Transfer at the Forward Stagnation Point of Blunt Bodies," NACA TN 3513, July 1955.

NASA-Langley, 1963 M103

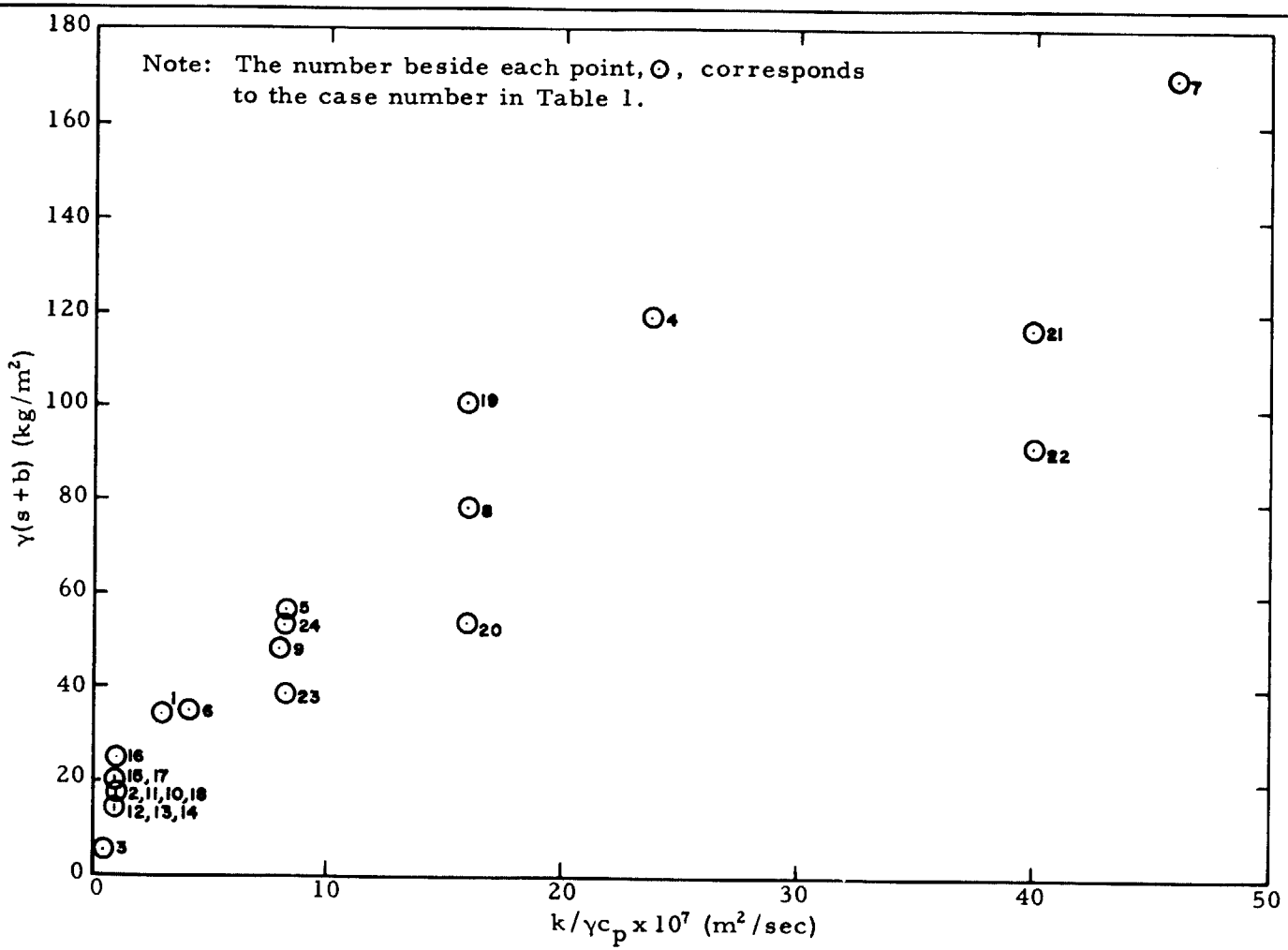

FIG. 9. THE NECESSARY WEIGHT γ(s+b) AS A FUNCTION OF THE THERMAL DIFFUSIVITY FOR ALL THE CALCULATED GLASS SHIELDS